Interactions among the Three Structural Motifs of the C-Terminal Region of Human Thrombospondin-2

ARTICLE *in* BIOCHEMISTRY · JUNE 2003

Impact Factor: 3.02 · DOI: 10.1021/bi026983p · Source: PubMed

4 AUTHORS, INCLUDING:

Tina M Misenheimer
University of Wisconsin–Madison
20 PUBLICATIONS **687** CITATIONS
SEE PROFILE

Douglas S Annis
University of Wisconsin–Madison
68 PUBLICATIONS **2,190** CITATIONS
SEE PROFILE

Interactions among the Three Structural Motifs of the C-Terminal Region of Human Thrombospondin-2

Tina M. Misenheimer, Blue-leaf A. Hannah, Douglas S. Annis, and Deane F. Mosher*

Department of Medicine, University of Wisconsin-Madison, 1300 University Avenue, Madison, Wisconsin 53706

Received October 10, 2002; Revised Manuscript Received February 12, 2003

ABSTRACT: The C-terminal regions of thrombospondins (TSPs) contain three elements, EGF-like modules (E), a series of Ca^{2+}-binding repeats (Ca), and a C-terminal sequence (G). We have looked for interactions among these elements in four recombinant proteins based on human TSP-2: E3CaG-2, CaG-2, E3Ca-2, and Ca-2. When bound Ca^{2+} was assayed by atomic absorption spectroscopy or an equilibrium dialysis protocol in which Ca^{2+} was removed from the proteins prior to equilibrium dialysis, E3CaG-2 bound 22−27 Ca^{2+}, CaG-2 bound 17−20 Ca^{2+}, and E3Ca-2 and Ca-2 bound 14−20 Ca^{2+}. Approximately 10 of the bound Ca^{2+} in E3CaG-2 were exchangeable. The far UV circular dichroism (CD) spectrum of Ca^{2+}-replete E3CaG-2 contained a strong negative band at 203 nm attributable to Ca and a less intense negative band at 218 nm attributable to Ca and G. Chelation of Ca^{2+} with EDTA shifted the 203 nm band of all four proteins and the 218 nm band of E3CaG-2 and CaG-2 to less negative positions. The apparent EC50 for the far UV CD transition was 0.22 mM Ca^{2+} for all proteins, indicating that Ca^{2+} binding to Ca is primarily responsible for the CD change. Near UV CD and intrinsic fluorescence revealed that the tryptophan residues in G are sensitive to changes in Ca^{2+}. Differential scanning calorimetry of the proteins in 2 mM Ca^{2+} showed that E3CaG-2 melts with two transitions, 44−51 °C and 75−83 °C. The lower transition required G, while the higher transition required Ca. Both transitions were stabilized in constructs containing E3. These results indicate that E3, Ca, and G function as a complex structural unit, and that the structures of both Ca and G are influenced by the presence or absence of Ca^{2+}.

The thrombospondin (TSP)[1] family of extracellular glycoproteins consists of five members in vertebrates, TSP 1−4 and TSP-5/COMP (cartilage oligomeric matrix protein) (*1*−*5*), and a single member in *Drosophila*, dTSP (*6*, *7*). TSPs are modular multimeric proteins. The carboxy-terminal end of a monomer consists of three to six EGF-like domains (E); seven tandem aspartate-rich, Ca^{2+}-binding repeats (Ca); and an approximately 230-residue C-terminal sequence (G) (Figure 1). The Ca^{2+}-binding repeats and C-terminal sequence are spaced almost exactly the same in different TSPs and share many blocks of identical residues. Mutations in the Ca^{2+}-binding repeats and C-terminal sequence of TSP-5/COMP have been identified in patients with two syndromes of skeletal dysplasia, pseudoachondroplasia (PSACH) and multiple epiphyseal dysplasia (EDM1) (*8*−*14*). Also, a nonsynonymous single nucleotide polymorphism in the Ca^{2+}-binding region of TSP-1 has been linked to coronary heart disease (*15*).

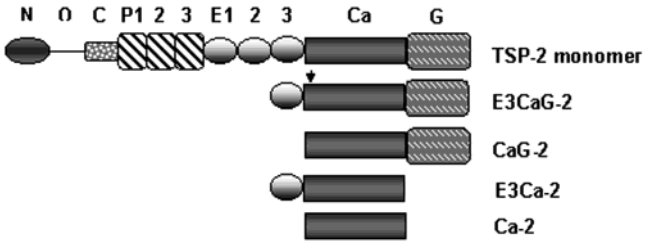

FIGURE 1: Schematic diagram of TSP-2 constructs. The N-terminal heparin binding domain (N), the oligomerization domain (O), three properdin domains (P1−3), three EGF-like domains (E1−3), the Ca^{2+}-binding repeats (Ca), and the C-terminal sequence (G) are indicated in the diagram of the TSP-2 monomer. The TSP-2 constructs used in the studies (E3CaG-2, CaG-2, E3Ca-2, and Ca-2) are also illustrated. An *arrow* marks the location of Trp 700 that is changed to Phe 700 in the construct E3CaG-2 W700F.

The presence of Ca^{2+} alters the structure and function of TSPs. Calcium-dependent functions include adhesion of cells to TSP-1 (*16*, *17*) and TSP-2 (*18*), inhibition of cathepsin G (*19*), and neutrophil elastase (*20*) by TSP-1, and reduction of von Willebrand factor by TSP-1 (*21*). Rotary shadowing has demonstrated structural changes in the presence of Ca^{2+} for TSP-1 (*22*−*24*) as well as for TSP-3, TSP-4, and TSP-5/COMP (*25*−*27*). Sedimentation velocity experiments of TSP-1 (*22*) and recombinant Ca^{2+}-binding repeats of TSP-5/COMP (*28*) revealed an increase in the sedimentation coefficient upon addition of Ca^{2+} which is consistent with a

* To whom correspondence should be addressed. Phone: (608) 262−1375. FAX: (608) 263−4969. E-mail: tmmisenh@facstaff.wisc.edu.

[1] Abbreviations: Ca-2, recombinant Ca^{2+}-binding repeats of TSP-2 (residues 693−947); CaG-2, recombinant C-terminal portion of TSP-2 from the Ca^{2+}-binding repeats to the end of TSP-2 (residues 693−1172); CD, circular dichroism; COMP, cartilage oligomeric matrix protein; DSC, differential scanning calorimetry; DTT, dithiothreitol; EGF, epidermal growth factor; E3Ca-2, recombinant C-terminal portion of TSP-2 from the third EGF-like module to the end of the Ca^{2+}-binding repeats of TSP-2 (residues 650−947); E3CaG-2, recombinant C-terminal portion of TSP-2 from the third EGF-like module to the end of TSP-2 (residues 650−1172); E3CaG-2 W700F, recombinant C-terminal portion of TSP-2 from the third EGF-like module to the end of TSP-2 (residues 650−1172) with W700 changed to F; EDM1, multiple epiphyseal dysplasia; G-2, recombinant C-terminal globule of TSP-2 (residues 947−1172); PSACH, pseudoachondroplasia; TSP, thrombospondin.

10.1021/bi026983p CCC: $25.00
Published on Web 04/05/2003

change in structure upon Ca^{2+}-binding. TSP-1 has been shown to interact with Ca^{2+} cooperatively (*29*, *30*) and to bind 35 ± 3 Ca^{2+} per trimer (approximately 12 Ca^{2+} per monomer) as assessed by equilibrium dialysis using Ca^{2+}-replete protein (*30*).

Examination of constructs based on TSP-2 has an advantage over the other TSPs because TSP-2 lacks an unpaired cysteine in the C-terminal region that has the potential to undergo thiol-disulfide isomerization (*31*). Previously, we expressed the C-terminal region of TSP-2 in insect cells, purified the expressed protein after secretion, demonstrated that the protein binds Ca^{2+}, and determined that the disulfide pairing of the 18 cysteines in Ca and G is sequential (*32*). The same disulfide pairing patterns were observed in E3CaG-2, constructs lacking E3 (CaG-2) or constructs lacking E3 and G (Ca-2). We could not purify G by itself and speculated that interactions between G and Ca may be required for proper folding of G in the secretory organelles. In this report, we describe biophysical properties of E3CaG-2, E3Ca-2, CaG-2, and Ca-2 (Figure 1). Alterations in Ca^{2+}-binding, far UV CD, near UV CD, intrinsic fluorescence and differential scanning calorimetry (DSC) demonstrate that G is affected by the presence of Ca^{2+} even though the proposed Ca^{2+}-binding sites lie within the adjacent Ca^{2+}-binding domain. The data indicate that G, Ca, and E3 interact with each other and fold and function as one structural unit.

MATERIALS AND METHODS

Expression and Purification of E3CaG-2, CaG-2, E3Ca-2, Ca-2, and E3CaG-2 W700F. The proteins were expressed using a baculovirus expression system and purified via nickel chelate chromatography as described previously (*32*−*34*). Briefly, DNA encoding the third EGF-like domain through the C-terminus of TSP-2 (residues 650−1172 of full-length TSP-2), E3CaG-2, was cloned into the baculovirus transfer vector pAcGP67.coco. Ca-2 (residues 693−947), CaG-2 (residues 693−1172), E3Ca-2 (residues 650−947), and E3CaG-2 W700F (residues 650−1172 with Trp in position 700 changed to Phe) were made using the E3CaG-2 plasmid for further rounds of PCR to allow insertion of altered constructs into pAcGP67.coco. E3CaG-2, CaG-2, E3Ca-2, Ca-2, and E3CaG-2 W700F were expressed by infecting High Five insect cells (Invitrogen) in SF900II serum-free media at 22 °C with high titer virus (>10^8 pfu/mL) at MOI = 5. Conditioned medium was collected approximately 65 h post-infection. His-tagged proteins were purified from the medium using Ni^{2+}-nitrilotriacetic acid resin (Qiagen) (*32*). The Ca^{2+} concentration of the final preparations was 2 mM. The highest production was observed for E3CaG-2 (39−75 mg/L), while the lowest production was observed for CaG-2 (18−25 mg/L). Protein concentration was determined using absorbance at 280 nm and calculated extinction coefficients of 1.33, 1.36, 0.593, 0.524, and 1.24 mL mg^{-1} cm^{-1} for E3CaG-2, CaG-2, E3Ca-2, Ca-2, and E3CaG-2 W700F, respectively (*35*).

Calcium Binding. The ability of purified proteins to bind Ca^{2+} was measured directly using equilibrium dialysis with $^{45}CaCl_2$ (Amersham Corp.) (*30*, *32*). Briefly, proteins (15−28 μM) were dialyzed into 10 mM MOPS, 150 mM NaCl, pH 7.5 containing 0−2 mM $CaCl_2$ plus $^{45}CaCl_2$ for 4 h at 22 °C using 10 000 MWCO microdialyzers (Pierce) in 48 well plates (Falcon). Pilot experiments demonstrated that the enrichment of $^{45}Ca^{2+}$ in the protein-containing compartment was complete by 3 h. In method 1, the protein was kept in buffer containing 2 mM Ca^{2+} up until initiation of equilibrium dialysis. In method 2, Ca^{2+} was removed from the proteins prior to equilibrium dialysis by addition of 4 mM EDTA followed by approximately 40 h of dialysis against five changes of 10 mM MOPS, 0.15 M NaCl, pH 7.5. After equilibrium dialysis, protein and buffer samples were analyzed for radioactivity, and protein concentration was determined using the BCA protein assay (Pierce).

Calcium content of the proteins was also quantified using a Solaar Unicam 969 flame atomic absorption spectrometer. Prior to analysis, protein (12−27 μM) previously in 2 mM Ca^{2+} was dialyzed into 10 mM MOPS, 150 mM NaCl, pH 7.5 containing 0.5 mM $CaCl_2$ overnight at 4 °C. Protein and dialysis buffer were analyzed for calcium using calcium carbonate as the standard.

Circular Dichroism. Circular dichroism (CD) studies were performed on an Aviv CD spectrometer, model 62A DS. Far UV measurements were taken at 25 °C in a 0.1-cm path length cuvette using protein (1−6 μM) dialyzed into 5 mM MOPS, 100 mM NaCl, 2 mM $CaCl_2$, pH 7.5. Near UV CD measurements were taken at 25 °C in a 1-cm path length cuvette using protein (10−35 μM) dialyzed into 10 mM MOPS, 150 mM NaCl, 2 mM $CaCl_2$, pH 7.5. Calcium titration results were analyzed by comparing the fractional change (R) in mean residue ellipticity (M) at 220 nm at a given calcium concentration divided by the difference in values observed when no further changes occur upon addition of EDTA; $R = (M_E - M)/(M_E - M_{ca})$ where M_E = mean residue ellipticity after 2 mM EDTA addition, and M_{ca} = mean residue ellipticity at 2 mM $CaCl_2$. The Hill equation that describes this plot is $\log(R/1 - R) = n\log[Ca^{2+}] + \log K$, where n is the Hill coefficient and K is an equilibrium dissociation constant (*29*).

Intrinsic Fluorescence. Fluorescence emission spectra of purified proteins (0.5−4.0 μM) in 5 mM MOPS, 100 mM NaCl, 2 mM $CaCl_2$, pH 7.5 were obtained at 25 °C with an SLM-8100C fluorimeter with excitation at 295 nm. Increasing amounts of EDTA were added directly to the cuvettes. Total tryptophan fluorescence intensities were obtained for each experiment by integrating the fluorescence spectra after baseline subtraction. Calcium titration results were analyzed by comparing the fractional change (R) in total fluorescence at a given calcium concentration (F) divided by the difference in values observed when no further changes occur upon addition of EDTA; $R = (F_E - F)/(F_E - F_{ca})$ where F_E = fluorescence after 2 mM EDTA addition, F_{ca} = fluorescence at 2 mM $CaCl_2$.

Calorimetry. Differential scanning calorimetry (DSC) was done using a Microcal differential scanning calorimeter with proteins (17−40 μM) dialyzed into 10 mM MOPS, 150 mM NaCl, 2 mM $CaCl_2$, pH 7.5. Scans were from 15 to 95 °C at a rate of 60 deg/h.

RESULTS

Calcium Binding. The ability of the four C-terminal TSP-2 constructs (Figure 1) to bind Ca^{2+} was quantified by equilibrium dialysis. When the proteins in 2 mM Ca^{2+} were dialyzed for 4 h at 22 °C with mixtures of 0−2 mM $CaCl_2$

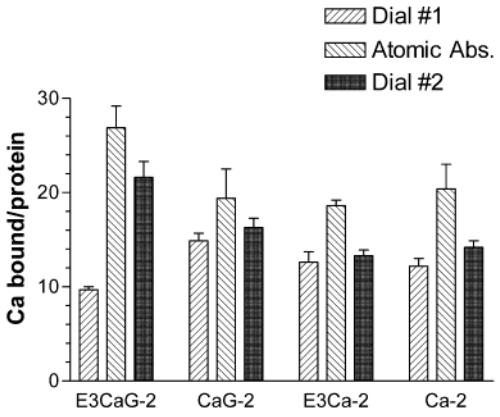

FIGURE 2: Calcium binding. Calcium enrichment was measured using equilibrium dialysis with ^{45}Ca or atomic absorption spectroscopy. Equilibrium dialysis and atomic absorption were done as described in Materials and Methods. Proteins assayed via equilibrium dialysis were either in 2 mM Ca^{2+} (Dial 1) or stripped of Ca^{2+} (Dial 2). Atomic absorption was done after dialysis of Ca^{2+}-replete protein into buffer containing 0.5 mM $CaCl_2$ (atomic abs.). Values are expressed as the mean ± SEM of 3−6 experiments.

plus $^{45}CaCl_2$ such that the final concentration of free Ca^{2+} was 0.25−2 mM (dialysis method 1), E3CaG-2 maximally bound 10 Ca^{2+}, whereas Ca-2 and E3Ca-2 bound 13 Ca^{2+} and CaG-2 bound 15 Ca^{2+} (Figure 2). The value for E3CaG-2 is similar to what was found with full-length platelet TSP-1 analyzed by the same dialysis method (*30*). To explain why E3CaG-2 bound less Ca^{2+} than the other proteins, we hypothesized that a fraction of Ca^{2+} bound to E3CaG-2 in 2 mM Ca^{2+} is not readily exchangeable. We, therefore, analyzed calcium levels in proteins by flame atomic absorption spectroscopy (Figure 2). Prior to atomic absorption spectroscopy, proteins in 2 mM Ca^{2+} were dialyzed into buffer containing 0.5 mM Ca^{2+}, a level at which maximal Ca^{2+}-binding was achieved using equilibrium dialysis (data not shown). The levels were significantly higher with atomic absorption than dialysis method 1 for all proteins, but most markedly so for E3CaG-2 (Figure 2). E3CaG-2 bound 27 ± 2 Ca^{2+} when measured by atomic absorption, whereas CaG-2, Ca-2, and E3Ca-2 bound approximately 19 Ca^{2+}. To evaluate further the hypothesis that Ca^{2+}-replete E3CaG-2 does not freely exchange all bound Ca^{2+} with the buffer during dialysis, equilibrium dialysis method 2 was done on protein stripped of Ca^{2+} by treatment with 4 mM EDTA followed by extensive dialysis into buffer without Ca^{2+} (Figure 2). The equilibrium dialysis result (22 ± 2 bound Ca^{2+}) for stripped E3CaG-2 was more similar to the result for atomic absorption spectroscopy of Ca^{2+}-replete E3CaG-2 than to equilibrium dialysis of Ca^{2+}-replete E3CaG-2. In contrast, Ca^{2+}-stripped Ca-2 and E3Ca-2 bound 14 Ca^{2+} and CaG-2 bound 17 Ca^{2+}, similar to equilibrium dialysis results with the Ca^{2+}-replete proteins (Figure 2). The result with Ca^{2+}-replete or Ca^{2+}-stripped Ca-2 is also very similar to results with nearly identical constructs from TSP-5/COMP that were purified in the absence of Ca^{2+} (*28*, *36*).

Far UV CD. The far UV CD spectra of E3CaG-2 and CaG-2 were similar in shape to those reported for full-length TSP-1 (*29*) with negative bands at 203 and 218 nm (Figure 3). The far UV CD spectra for E3Ca-2 and Ca-2 lacked the negative band at 218 nm and had more pronounced negative bands at 203 nm (−23200 and −19600 deg cm^2/decimol, respectively) compared to the 203 nm bands for E3CaG-2 and CaG-2 (−14200 and −12200 deg cm^2/decimol, respectively). The SOPM program for secondary structure prediction (*37*, *38*) predicts 2% α-helix, 22% β-structure, and 76% coil for Ca-2 and 12% α-helix, 42% β-structure, and 46% coil for G-2. Assuming no interactions between G and E3Ca, the spectrum for G can be calculated by subtraction of the expected contribution of E3Ca-2 (55.2% based on relative masses) from the observed E3CaG-2 spectrum. The resulting G-2 spectrum is dominated by a band with a minimum at 218 nm which is compatible with the predicted increased β-structure (Figure 3A). When the expected contribution of Ca-2 (51.5% of CaG-2 based on relative masses) is subtracted from the observed CaG-2 spectrum, the deduced spectrum for G-2 also contained the 218 nm band (Figure 3B).

Ca^{2+} chelation by the addition of EDTA shifted the spectra of all four proteins to less negative positions (Figures 3C,D) as was observed for full-length TSP-1 (*29*). The effects of Ca^{2+} were titrated by monitoring the change in ellipticity at 220 nm upon addition of increasing amounts of EDTA (Figure 3E). All the proteins had similar titration curves with EC50s around 0.22 mM Ca^{2+} and Hill coefficients of 3 (Figure 3F), indicating that Ca^{2+} binding cooperatively affects the far UV CD spectra similarly regardless of whether E3 or G are present along with Ca.

Near UV CD. E3CaG-2 and CaG-2 have eight tryptophans, seven in G and one in Ca near its juncture with E3 (Trp 700). Comparison of near UV CD spectra of E3CaG-2 and CaG-2 to E3Ca-2 and Ca-2, therefore, should give insight on how the different modules interact during Ca^{2+} binding. Near UV CD spectra of E3CaG-2 and CaG-2 in 2 mM Ca^{2+} contained a positive band at 292 nm (Figure 3A,C) that can be attributed to the transition of tryptophans (*39*). Near UV CD of Ca-2 in 2 mM Ca^{2+} (Figure 4D) did not contain a band at 292 nm, suggesting that the 292 nm band arises from tryptophans in G. To localize further the responsible tryptophan(s) in E3CaG-2, E3CaG-2 W700F was made in which Phe replaced Trp 700 in the Ca region. It should be noted that the residue homologous to Trp 700 is Tyr in TSP-3 and TSP-4 and Phe in TSP-5/COMP (*40*). The near UV CD spectrum of the W700F mutant in 2 mM Ca^{2+} also contained the positive band at 292 nm (Figure 4B). Therefore, one or several of the seven tryptophans in G must be responsible for the 292 nm band. Addition of EDTA resulted in loss of the peak at 292 nm (Figure 4), indicating that the tryptophans in G are sensitive to chelation of Ca^{2+}.

Fluorescence Spectroscopy. The local environment of the tryptophans was examined further by intrinsic fluorescence after excitation at 295 nm (Figure 5). The fluorescence emission spectra for E3CaG-2, CaG-2, and E3CaG-2 W700F were similar to each other (Figure 5A,B,E). Peak emission (λmax) was 333−336 nm in 2 mM Ca^{2+} and red-shifted to 340 nm after addition of 2 mM EDTA. EDTA addition also decreased the fluorescence intensity of the proteins. The fact that E3CaG-2 W700F exhibited the same spectra as E3CaG-2 indicates that intrinsic fluorescence is dominated by the remaining seven tryptophans in G. The fluorescence emission spectra of E3Ca-2 and Ca-2 which have only one tryptophan, Trp 700, had less fluorescence intensity and a λmax in 2 mM Ca^{2+} of 339 nm in E3Ca-2 and 345 nm in Ca-2. The different λmax indicate that the local environment of Trp 700 is influenced by the presence of E3 such that it is more hydrophilic in the absence of E3. Addition of EDTA shifted

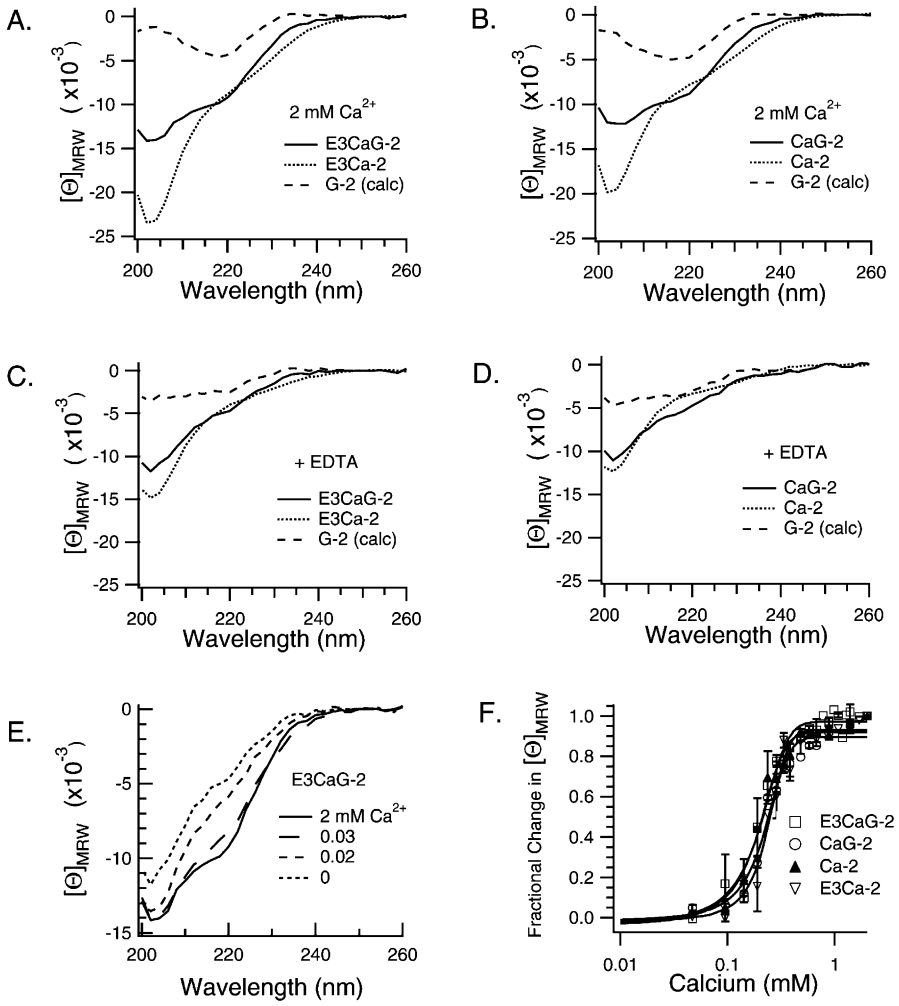

FIGURE 3: Far UV circular dichroism. Far UV CD spectra for E3CaG-2, E3Ca-2, CaG-2, and Ca-2 were measured at 25 °C in 5 mM MOPS, 100 mM NaCl, pH 7.5 in the presence of 2 mM Ca^{2+} (A and B) or after addition of 2 mM EDTA to remove Ca^{2+} (C and D). Representative spectra are shown expressed as residue ellipticity, $[\Theta]_{MRW}$, (deg cm^2/decimol). Spectra for G-2 were predicted after subtraction of 55.2% E3Ca-2 (relative mass) from the observed E3CaG-2 spectrum (A and C) or after subtraction of 51.5% Ca-2 (relative mass) from the observed CaG-2 spectrum (B and D). Representative spectra (2.0, 0.3, 0.02, and 0 mM $CaCl_2$) are shown for the titration of E3CaG-2 with EDTA (E). Titration curves for E3CaG-2, CaG-2, Ca-2, and E3Ca-2 (F) were made by addition of increasing amounts of EDTA and calculation of the fractional change in ellipticity at 220 nm at different Ca^{2+} levels as described in Materials and Methods.

the λmax of both E3Ca-2 and Ca-2 to 352 nm but increased the fluorescence intensities rather than causing a decrease as in E3CaG-2.

The effect of Ca^{2+} on the tryptophan environments was examined further by titrating the proteins with increasing amounts of EDTA to remove the Ca^{2+}. The fluorescence titration curves were different for the different proteins. The apparent EC50s for E3CaG-2, E3Ca-2, and Ca-2 were 0.80, 0.36, and 0.60 mM Ca^{2+}, respectively (Figure 5F). CaG-2 and E3CaG-2 W700F exhibited complex titrations. Upon addition of EDTA, the fluorescence intensities decreased to a minimum when the Ca^{2+} concentration was lowered to about 0.7 mM (CaG-2) or 0.4 mM (E3CaG-2 W700F) and then increased as Ca^{2+} was lowered further. The λmax, however, shifted monotonically from 335 to 340 nm. Comparison of E3Ca-2 to Ca-2 indicates that the presence of E3, as well as causing alterations in the fluorescence spectra of Trp 700, shifted the apparent EC50 to lower Ca^{2+} levels. The alterations in the fluorescence spectrum of E3CaG-2 and E3CaG-2 W700F upon removal of Ca^{2+} indicate that the tryptophans in G are affected by the presence of Ca^{2+} and correlate with the near UV CD analyses.

Differential Scanning Calorimetry. In 2 mM Ca^{2+}, E3CaG-2 melted with two transitions, 50.5 and 82.7 °C (Figure 6). CaG-2 also melted with two transitions, but the temperatures, 44.7 and 77.5 °C, were lower than those observed for E3CaG-2. E3Ca-2, and Ca-2 melted with one transition at 81.5 and 75.3 °C, respectively. The 82.7 °C transition in E3CaG-2 was, therefore, due to the Ca^{2+}-binding region, Ca, while the 50.5 °C transition required the presence of G. Comparisons of E3Ca-2 to Ca-2 and E3CaG-2 to CaG-2 reveal that the presence of E3 stabilizes the proteins, resulting in a 5−6 °C increase in melting temperatures of both transitions. The lower temperature transition was completely irreversible, and the higher temperature transition was only partially reversible (Figure 6). The irreversibility of the first transition alone was tested by heating E3CaG-2 to 65 °C twice. Under these conditions, the transition was irreversible (data not shown). In 0.3 mM $CaCl_2$, the two transitions for E3CaG-2 were shifted to 42.5 and 66.6 °C (data not shown). Upon addition of 2 mM EDTA to chelate Ca^{2+}, all proteins were very unstable to heating. Very little signal could be measured for E3Ca-2 or Ca-2 after EDTA addition (data not shown). A small peak at 43 °C was observed for CaG-2 and

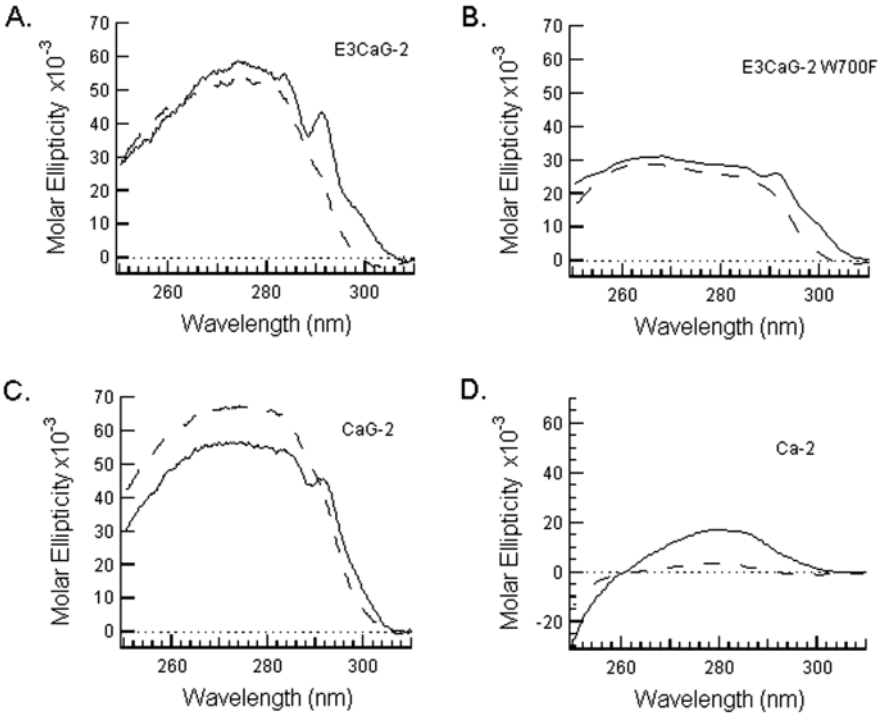

FIGURE 4: Near UV circular dichroism. Near UV CD spectra of E3CaG-2 (A), E3CaG-2 W700F (B), CaG-2 (C), and Ca-2 (D) were measured at 25 °C in the presence (−) and absence (- -) of 2 mM Ca^{2+} in 10 mM MOPS, 150 mM NaCl, pH 7.5. Calcium was removed by addition of 2 mM EDTA. Representative spectra are shown expressed as molar ellipticity (deg cm^2/decimol).

E3CaG-2 with nothing at the higher temperature (data not shown).

DISCUSSION

We have expressed the Ca^{2+}-binding module, Ca-2, of TSP-2 with and without the preceding EGF-like E3 module and C-terminal G sequence in insect cells using a baculovirus system. Analyses of these proteins revealed several classes of binding sites for Ca^{2+} and evidence of interactions among E3, Ca, and G.

When proteins were stripped of Ca^{2+} prior to equilibrium dialysis, CaG-2, Ca-2, and E3Ca-2 bound 14−17 Ca^{2+}, whereas E3CaG-2 bound 22 Ca^{2+} (Figure 2). Atomic absorption data were similar to the trends seen with equilibrium dialysis of Ca^{2+}-stripped proteins, but an additional 5 mol Ca^{2+} per mole protein were estimated using atomic absorption spectroscopy. Consistent with our data obtained using Ca^{2+}-stripped protein (dialysis method 2), Ca of TSP-5/COMP that was purified in the absence of Ca^{2+} was found to bind 17 Ca^{2+} (*28*) or 14 Ca^{2+} (*36*) using equilibrium dialysis. Thus, the data indicate that inclusion of G alongside E3Ca results in 5−8 more binding sites for Ca^{2+}.

Upon equilibrium dialysis of Ca^{2+}-replete proteins, only 10 binding sites were found on E3CaG-2 as compared to 13 for Ca-2 and E3Ca-2 and 15 for CaG-2. These results suggest that Ca^{2+} not freely exchangeable with solution during dialysis must be associated with Ca^{2+}-replete E3CaG-2. The presumptive Ca^{2+}-binding consensus sequence DXDX-DXXGDXXDX occurs 13 times in the Ca module of a TSP monomer. Ca^{2+}-binding, however, is apparently more complex than simply binding to those 13 sequences. Ca-2 bound 15 Ca^{2+} as measured via dialysis using Ca^{2+} -stripped protein, Addition of G or E3 to Ca-2 to make E3Ca-2 or CaG-2 did not significantly change the Ca^{2+} binding numbers, but the presence of both G and E3 in E3CaG-2 greatly accentuated the differences between bound and exchangeable Ca^{2+} with 22 Ca^{2+} observed via dialysis using Ca^{2+}-stripped protein versus 10 Ca^{2+} bound via dialysis using Ca^{2+}-replete protein. The G module must, therefore, interact with both E3 and Ca in some manner to create more Ca^{2+}-binding sites, but fewer sites for exchangeable Ca^{2+} (Figure 7). In proteins containing EF-hands, Ca^{2+} is coordinated by six residues, five of which usually have an oxygen-containing side chain (*41*, *42*). The oxygen from the main chain coordinates the sixth position. In Ca-2, 13 sequences have features of EF-hands (*32*). Of the 225 residues in G-2, 48 have potential coordinating side chains (10 Asn, 17 Asp, 12 Gln, and 9 Glu). Twenty-seven of these 48 residues are completely conserved among the five vertebrate TSPs. These residues may contribute to the 5−8 extra Ca^{2+}-binding sites observed in E3CaG-2 and to the creation of the non-dissociable sites deduced to be present in E3CaG-2 (Figure 7).

Spectroscopy was used to examine the protein structures in the presence and absence of Ca^{2+}. Far UV CD revealed that the structures of the proteins were affected similarly upon removal of Ca^{2+} (Figure 3). Ca-2 has intense negative ellipticity at 203 nm that is diluted out by apparent β-structure in G. Intrinsic fluorescence revealed that removal of Ca^{2+} made the local tryptophan environments more hydrophilic in all the proteins as indicated by increases in the λmax. This effect was greater for Trp 700 (Figure 5C,D) than for the tryptophan residues in G (Figure 5A,B,E). Titrations of tryptophan fluorescence were different among proteins and occurred at higher Ca^{2+} levels than changes in far UV CD (Figures 3 and 5). The presence of E3 stabilized the local environment of Trp 700 such that the apparent EC50 for titration of fluorescence was 0.36 mM Ca^{2+} for E3Ca-2

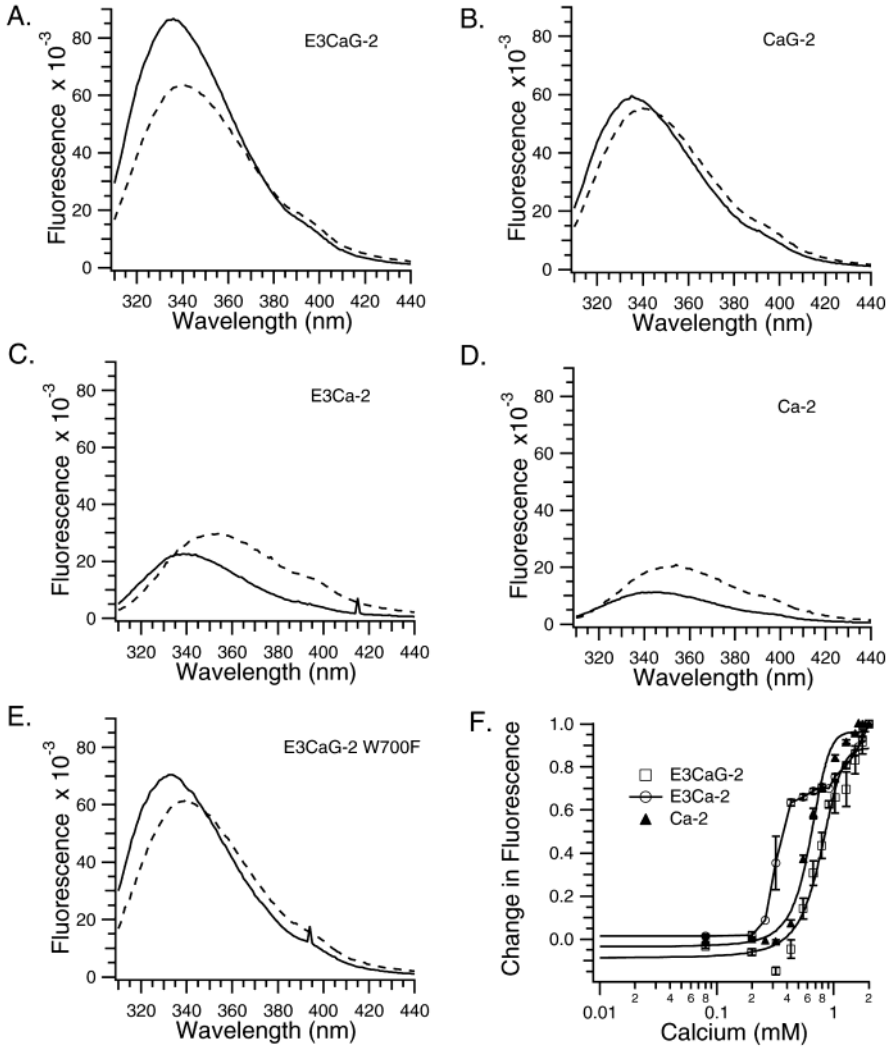

FIGURE 5: Intrinsic fluorescence. Intrinsic fluorescence spectra of E3CaG-2 (A), CaG-2 (B), E3Ca-2 (C), Ca-2 (D), and E3CaG-2 W700F (E) were measured at 25 °C in the presence (−) and absence (- -) of 2 mM Ca^{2+} in 5 mM MOPS, 100 mM NaCl, pH 7.5 after excitation at 295 nm. Calcium was removed by addition of 2 mM EDTA. Representative spectra are shown expressed as relative fluorescence intensity. Protein concentrations were 0.6 to 4 μM. Titration curves for E3CaG-2, E3Ca-2, and Ca-2 (F) were made by addition of increasing amounts of EDTA and calculation of the fractional change in fluorescence intensity at different Ca^{2+} levels as described in Materials and Methods.

versus 0.60 mM Ca^{2+} for Ca-2 (Figure 5). Upon removal of Ca^{2+}, fluorescence intensity of E3CaG-2 W700F was decreased, and the λmax was shifted from 333 to 340 nm indicating that the tryptophans in G are sensitive to the presence of Ca^{2+}. Near UV CD revealed that a 292 nm band attributable to the tryptophans in G is sensitive to the presence of Ca^{2+} (Figure 4). Overall, the spectroscopy data indicate the adjacent E3 and G modules interact with Ca and that binding of Ca^{2+} affects the structures of both G and Ca.

DSC to examine how the presence of E3 and G affect the thermal stability of the proteins revealed two transitions. Both transitions were observed upon heating E3CaG-2 and CaG-2, whereas only the second transition was observed for E3Ca-2 and Ca-2 (Figure 6). This difference indicates that the higher melting point near 80° is due to Ca. We were unable to express G-2 by itself using the baculovirus expression system (*32*). Similar problems were encountered by Adams and Lawler using GST fusion proteins expressed in bacteria (*43*). They expressed the latter part of the type 3 repeats with G instead of G alone because of stability problems. These observations indicate that G-2 probably does not fold properly without Ca-2. Therefore, the lower melting point near 50 °C may be due to the unfolding of the interface between Ca and G rather than the unfolding of G per se. Comparison of E3Ca-2 to Ca-2 and E3CaG-2 to CaG-2 revealed that the presence of E3 stabilized the proteins resulting in a 5−6 °C increase in melting temperatures of both transitions. Therefore, E3 increased the stability of both G and Ca. The presence of Ca^{2+} also stabilized the protein. The E3CaG-2 transitions at 50.5 and 82.7 °C in 2 mM $CaCl_2$ shifted to 42.5 and 66.6 °C in 0.3 mM $CaCl_2$, and complete Ca^{2+} chelation destabilized the entire region. The calorimetry data, therefore, support the spectroscopic evidence that the E3, Ca, and G portions of TSP-2 interact with one another and are responsive to the binding of Ca^{2+} to the Ca^{2+}-binding repeats of Ca.

The irreversibility of the denaturation upon heating of the C-terminal constructs suggests that molecular chaperones in the endoplasmic reticulum are required to facilitate optimal folding (*44*). TSP-1 has been found to complex with chaperones in the endoplasmic reticulum (*45*), and chaperones are associated with retained TSP-5/COMP in PSACH chondrocytes (*46*, *47*).

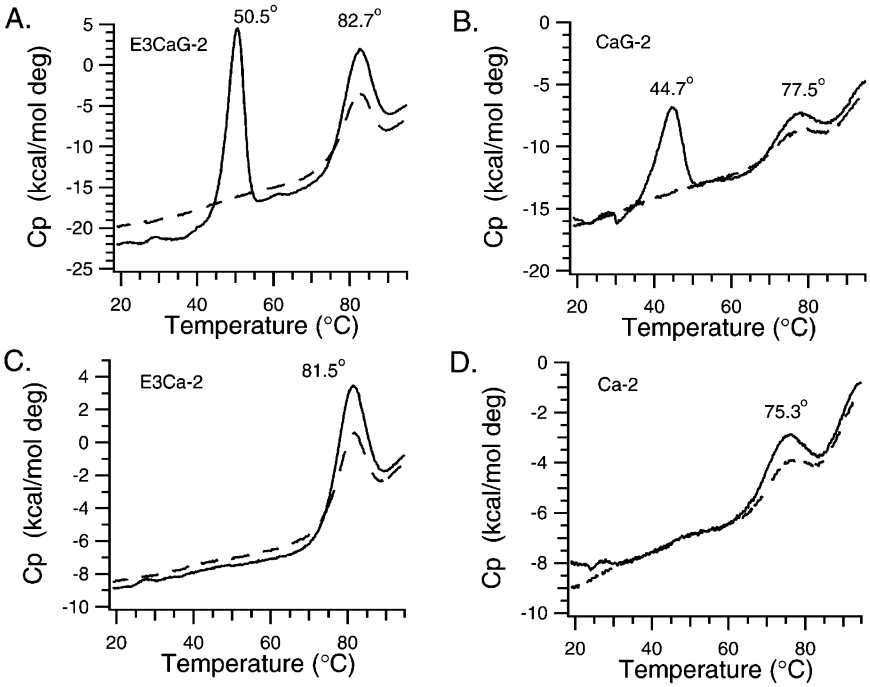

FIGURE 6: Differential scanning calorimetry. Thermal melting curves were measured for E3CaG-2 (A), CaG-2 (B), E3Ca-2 (C), and Ca-2 (D) in 10 mM MOPS, 150 mM NaCl, 2 mM $CaCl_2$, pH 7.5 using DSC. A second scan (- -) was done immediately after the first scan (−) to determine reversibility of the process.

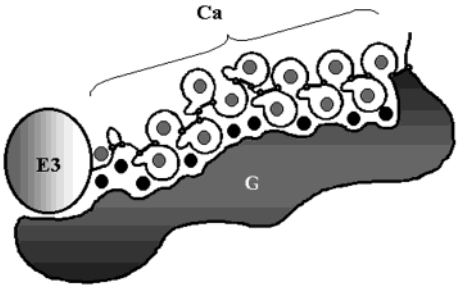

FIGURE 7: Model of calcium binding to E3CaG-2. A proposed model of the Ca^{2+}-replete form of E3CaG-2 is presented. Ca is represented by its disulfide bonded structure (*32*) where the disulfides are indicated by the *thick lines* connecting the *open circles* that represent the cysteines. E3 is represented by the *large oval* while G is represented by the *large amorphous shape*. The *gray circles* represent the exchangeable Ca^{2+} bound to the Ca^{2+}-binding type 3 repeats, while the *black circles* represent the nonexchangeable Ca^{2+} bound at the interface between G and E3Ca.

TSP-1 and TSP-2 are usually depicted as a trimer with three smaller N-terminal globules grouped together and linked by stalks to larger C-terminal globules. Rotary shadowing has demonstrated that, in the presence of Ca^{2+}, the C-terminal portion of TSP-1 enlarges while the stalk connecting the oligomerization domain to the C-terminal globule shortens (*22*−*24*). This structural change was also observed for TSP-3, TSP-4, and TSP-5/COMP (*25*−*27*). Our data indicate this observed structural change is explained by Ca^{2+}-binding causing a cooperative change in the entire E3CaG region. The stalk likely shortens upon binding of Ca^{2+} because G folds over Ca to reach E3 (Figure 7).

Understanding the complex structure of the C-terminal region of TSPs is important for understanding the mechanisms of skeletal dysplasias that are linked to mutations in Ca (*8*, *9*, *12*, *13*) and G (*10*, *11*, *13*, *14*) regions of TSP-5/COMP, and to coronary heart disease that is linked to a nonsynonymous single nucleotide polymorphism in Ca of TSP-1 (*15*). Two TSP-5/COMP mutations have been examined in constructs similar to our Ca construct and found to cause decreased Ca^{2+}-binding based on equilibrium dialysis (*27*, *28*). One proposed mechanism by which the TSP-5/COMP mutations cause disease is accumulation of unstable protein intracellularly (*48*−*50*). Our data indicate E3CaG folds as a complex structural unit such that Ca^{2+}-binding affects the structures of both Ca and G. These data are compatible with the observation that mutations in both the Ca and G regions of TSP-5/COMP cause the same disease phenotype.

ACKNOWLEDGMENT

This work was supported by funds from National Institutes of Health Grant HL54462. Instrument data were obtained at the University of Wisconsin-Madison Biophysics Instrumentation Facility, which is supported by the University of Wisconsin-Madison and National Science Foundation (NSF) Grant S10 RR1370. Ms. Hannah is a recipient of a predoctoral fellowship from the American Heart Association (Grant 0215322Z).

REFERENCES

1. Bornstein, P., O'Rourke, K., Wikstrom, K., Wolf, F. W., Katz, R., Li, P., and Dixit, V. M. (1991) *J. Biol. Chem. 266*, 12821−4.
2. LaBell, T. L., Milewicz, D. J., Disteche, C. M., and Byers, P. H. (1992) *Genomics 12*, 421−9.
3. Vos, H. L., Devarayalu, S., de Vries, Y., and Bornstein, P. (1992) *J. Biol. Chem. 267*, 12192−6.
4. Lawler, J., Duquette, M., Whittaker, C. A., Adams, J. C., McHenry, K., and DeSimone, D. W. (1993) *J. Cell Biol. 120*, 1059−67.
5. Oldberg, A., Antonsson, P., Lindblom, K., and Heinegard, D. (1992) *J. Biol. Chem. 267*, 22346−50.
6. Adams, J. C., Tucker, R. P., Lawler, J. (1995) The Thrombospondin Gene Family, R. G. Landes Company, Austin, TX.
7. Adolph, K. W. (2001) *Gene 269*, 177−84.

8. Briggs, M. D., Hoffman, S. M., King, L. M., Olsen, A. S., Mohrenweiser, H., Leroy, J. G., Mortier, G. R., Rimoin, D. L., Lachman, R. S., and Gaines, E. S. (1995) *Nat. Genet. 10*, 330−6.
9. Hecht, J. T., Nelson, L. D., Crowder, E., Wang, Y., Elder, F. F., Harrison, W. R., Francomano, C. A., Prange, C. K., Lennon, G. G., Deere, M., and Lawler, J. (1995) *Nat. Genet. 10*, 325−9.
10. Briggs, M. D., Mortier, G. R., Cole, W. G., King, L. M., Golik, S. S., Bonaventure, J., Nuytinck, L., De Paepe, A., Leroy, J. G., Biesecker, L., Lipson, M., Wilcox, W. R., Lachman, R. S., Rimoin, D. L., Knowlton, R. G., and Cohn, D. H. (1998) *Am. J. Hum. Genet. 62*, 311−9.
11. Deere, M., Sanford, T., Ferguson, H. L., Daniels, K., and Hecht, J. T. (1998) *Am. J. Med. Genet. 80*, 510−3.
12. Ikegawa, S., Ohashi, H., Nishimura, G., Kim, K. C., Sannohe, A., Kimizuka, M., Fukushima, Y., Nagai, T., and Nakamura, Y. (1998) *Hum. Genet. 103*, 633−8.
13. Deere, M., Sanford, T., Francomano, C. A., Daniels, K., and Hecht, J. T. (1999) *Am. J. Med. Genet. 85*, 486-90.
14. Holden, P., Meadows, R. S., Chapman, K. L., Grant, M. E., Kadler, K. E., and Briggs, M. D. (2001) *J. Biol. Chem. 276*, 6046−55.
15. Topol, E. J., McCarthy, J., Gabriel, S., Moliterno, D. J., Rogers, W. J., Newby, L. K., Freedman, M., Metivier, J., Cannata, R., O'Donnell, C. J., Kottke-Marchant, K., Murugesan, G., Plow, E. F., Stenina, O., and Daley, G. Q. (2001) *Circulation 104*, 2641−4.
16. Lawler, J., Weinstein, R., and Hynes, R. O. (1988) *J. Cell Biol. 107*, 2351−61.
17. Sun, X., Skorstengaard, K., and Mosher, D. F. (1992) *J. Cell Biol. 118*, 693−701.
18. Chen, H., Sottile, J., O'Rourke, K. M., Dixit, V. M., and Mosher, D. F. (1994) *J. Biol. Chem. 269*, 32226−32.
19. Hogg, P. J., Owensby, D. A., and Chesterman, C. N. (1993) *J. Biol. Chem. 268*, 21811−8.
20. Hogg, P. J., Owensby, D. A., Mosher, D. F., Misenheimer, T. M., and Chesterman, C. N. (1993) *J. Biol. Chem. 268*, 7139−46.
21. Xie, L., Chesterman, C. N., and Hogg, P. J. (2001) *J. Exp. Med. Sci. 193*, 1341−9.
22. Lawler, J., Chao, F., and Cohen, C. (1982) *J. Biol. Chem. 257*, 12257−12265.
23. Galvin, N. J., Dixit, V. M., O'Rourke, K. M., Santoro, S. A., Grant, G. A., and Frazier, W. A. (1985) *J. Cell Biol. 101*, 1434−41.
24. Lawler, J., Derick, L. H., Connolly, J. E., Chen, J. H., and Chao, F. C. (1985) *J. Biol. Chem. 260*, 3762−72.
25. Qabar, A., Derick, L., Lawler, J., and Dixit, V. (1995) *J. Biol. Chem. 270*, 12725−9.
26. Lawler, J., McHenry, K., Duquette, M., and Derick, L. (1995) *J. Biol. Chem. 270*, 2809−14.
27. Chen, H., Deere, M., Hecht, J. T., and Lawler, J. (2000) *J. Biol. Chem. 275*, 26538−44.
28. Maddox, B. K., Mokashi, A., Keene, D. R., and Bachinger, H. P. (2000) *J. Biol. Chem. 275*, 11412−7.
29. Lawler, J., and Simons, E. R. (1983) *J. Biol. Chem. 258*, 12098−101.
30. Misenheimer, T. M., and Mosher, D. F. (1995) *J. Biol. Chem. 270*, 1729−33.
31. Speziale, M. V., and Detwiler, T. C. (1990) *J. Biol. Chem. 265*, 17859−67.
32. Misenheimer, T. M., Hahr, A. J., Harms, A. C., Annis, D. S., and Mosher, D. F. (2001) *J. Biol. Chem. 276*, 45882−7.
33. Misenheimer, T. M., Huwiler, K. G., Annis, D. S., and Mosher, D. F. (2000) *J. Biol. Chem. 275*, 40938−45.
34. Mosher, D. F., Huwiler, K. G., Misenheimer, T. M., and Annis, D. S. (2002) *Methods Cell Biol. 69*, 69−81.
35. Mach, H., Middaugh, C. R., and Lewis, R. V. (1992) *Anal. Biochem 200*, 74−80.
36. Thur, J., Rosenberg, K., Nitsche, D. P., Pihlajamaa, T., Ala-Kokko, L., Heinegard, D., Paulsson, M., and Maurer, P. (2001) *J. Biol. Chem. 276*, 6083−92.
37. Geourjon, C., and Deleage, G. (1994) *Protein Eng. 7*, 157−64.
38. Combet, C., Blanchet, C., Geourjon, C., and Deleage, G. (2000) *Trends Biochem. Sci. 25*, 147−50.
39. Mach, H., Middaugh, C. R., and Denslow, N. (1995) in *Current Protocols in Protein Science* (Coligan, J. E., Ed.) John Wiley and Sons, Inc.
40. Adams, J. C., Monk, R., Taylor, A. L., Ozbek, S., Fascetti, N., Baumgartner, S., and Engel, J. (2003) *J. Mol. Biol.*, in press.
41. Moncrief, N. D., Kretsinger, R. H., and Goodman, M. (1990) *J. Mol. Evol. 30*, 522−62.
42. McPhalen, C. A., Strynadka, N. C., and James, M. N. (1991) *Adv. Protein Chem. 42*, 77−144.
43. Adams, J. C., and Lawler, J. (1994) *Mol. Biol. Cell 5*, 423−37.
44. Kuznetsov, G., and Nigam, S. K. (1998) *N. Engl. J. Med. 339*, 1688−95.
45. Kuznetsov, G., Chen, L. B., and Nigam, S. K. (1997) *J. Biol. Chem. 272*, 3057−63.
46. Hecht, J. T., Hayes, E., Snuggs, M., Decker, G., Montufar-Solis, D., Doege, K., Mwalle, F., Poole, R., Stevens, J., and Duke, P. J. (2001) *Matrix Biol. 20*, 251−62.
47. Vranka, J., Mokashi, A., Keene, D. R., Tufa, S., Corson, G., Sussman, M., Horton, W. A., Maddox, K., Sakai, L., and Bachinger, H. P. (2001) *Matrix Biol. 20*, 439−50.
48. Maddox, B. K., Keene, D. R., Sakai, L. Y., Charbonneau, N. L., Morris, N. P., Ridgway, C. C., Boswell, B. A., Sussman, M. D., Horton, W. A., Bachinger, H. P., and Hecht, J. T. (1997) *J. Biol. Chem. 272*, 30993−7.
49. Hecht, J. T., Montufar-Solis, D., Decker, G., Lawler, J., Daniels, K., and Duke, P. J. (1998) *Matrix Biol. 17*, 625−33.
50. Delot, E., Brodie, S. G., King, L. M., Wilcox, W. R., and Cohn, D. H. (1998) *J. Biol. Chem. 273*, 26692−7.

BI026983P